Longitudinal Auditory Pathophysiology Following Mild Blast Induced Trauma

Emily X. Han[1,2], Joseph M. Fernandez[2,3], Caitlin Swanberg[2], Riyi Shi[2,3], Edward L. Bartlett[1,3]

[1]Dept. of Biological Sciences, College of Science, Purdue University, West Lafayette, IN

[2]Weldon School of Biomedical Engineering, Purdue University, West Lafayette, IN

[3]Dept. Basic Medical Sciences, College of Veterinary Medicine, Purdue University, West Lafayette, IN

Correspondence should be addressed to Edward Bartlett (ebartle@purdue.edu)。

Department of Biological Sciences and

The Weldon School of Biomedical Engineering

206 S. Martin Jischke Dr.

Purdue University

West Lafayette, Indiana 47907-1791

Keywords: auditory brainstem response, envelope following response, neurodegeneration, auditory evoked potentials,

Abstract

Blast-induced hearing difficulties affect thousands of veterans and civilians. The long-term impact of even a mild blast exposure on the central auditory system (CAS) is hypothesized to contribute to many lasting behavioral complaints associated with mild blast traumatic brain injury (bTBI). Although recovery from mild blast has been studied over different time windows, few, if any, studies have investigated recovery longitudinally over short-term and longer-term (months) time windows. Specifically, many peripheral measures of auditory function either recover almost fully or exhibit subclinical deficits, thus masking deficits in processing complex, real-world stimuli that may recover with different time courses. Thus, examining the acute time course and pattern of neurophysiological impairment using appropriate stimuli is critical to better understanding and intervention of bTBI-induced auditory system impairments. In this study, we compared auditory brainstem response, middle-latency auditory evoked potentials, and envelope following responses. Stimuli were clicks, tone pips, amplitude modulated tones in quiet and in noise, and speech-like stimuli (iterated rippled noise pitch contours) in adult male rats subjected to mild blast and sham exposure over the course of two months. We found that blast animals demonstrated drastic threshold increases and auditory transmission deficits immediately after blast exposure, followed by substantial recovery during the window of 7-14 days post-blast, though with some deficits remaining even after two months. Challenging conditions and speech-like stimuli can better elucidate mild bTBI-induced auditory deficit during this period. Our results indicated multiphasic recovery, suggesting

different time windows for treatment, and deficits can be best observed using a small battery of sound stimuli.

Introduction

Hearing loss stands out as one of the most commonly reported consequences following blast injuries and can last for months or even years without significant external injury (Cohen et al., 2002; Cave et al., 2007; Ritenour et al., 2008; Saunders et al., 2015). Hearing difficulties have been hypothesized to contribute to many behavioral complaints associated with mild blast traumatic brain injury (Gallun et al., 2012b; Vander Werff, 2012). Most studies regarding blast-induced hearing loss have focused on damage in different parts of the peripheral auditory system (PAS) (Kerr, 1980; DePalma et al., 2005). However, significant hearing difficulties can occur in the absence of peripheral diagnostic indicators such as eardrum rupture or clinical threshold shifts (hearing loss >25 dB), indicating potential disruptions further upstream (Remenschneider et al., 2014; Saunders et al., 2015; Van Haesendonck et al., 2018). Increasing clinical (Berger et al., 1997; Cohen et al., 2002; Cave et al., 2007; Ritenour et al., 2008; Lew et al., 2009; Gallun et al., 2012a) and laboratory (Patterson and Hamernik, 1997; Ewert et al., 2012; Cho et al., 2013b; Du et al., 2013; Masri et al., 2018) evidence suggest that both peripheral and central auditory system (CAS) are important blast-susceptible structures, where CAS includes the brainstem, midbrain, thalamus, and cortex.

Subcortical CAS such as the auditory brainstem may be particularly vulnerable to blast injury, including hemorrhages, intracranial deformation and blood-brain barrier (BBB) permeability, glutamate excitotoxicity, elevated calcium, as well as elevated markers of oxidative stress and neuroinflammation from near short-term (1-7 days) up to 2

weeks (Knudsen and Øen, 2003; Leung et al., 2008; Säljö et al., 2011; Cho et al., 2013a; Song et al., 2015; Walls et al., 2016; Laplaca et al., 1997; Hamann et al., 2008)). Functional changes, such as spontaneous hyperactivity in the auditory brainstem (Luo et al., 2014a, 2014b), as well as structural changes in OHC loss (Ewert et al., 2012), axonal integrity, white matter changes in the inferior colliculus (IC) and auditory thalamus (Mao et al., 2012a), have been shown post-blast at various time points, from 24 hours, 7 days up to 2-3 weeks. Most of these previous studies only assessed one or two time points post-blast. Given the likelihood of multiple phases of primary and secondary blast-induced damage and their corresponding anatomical and electrophysiological changes, understanding the trajectory of post-blast recovery can help to identify critical time points and to direct therapies that are matched to the recovery mechanisms at those time points.

Clinical reports have suspected "hidden hearing loss" in blast-exposed veterans due to deficits in suprathreshold auditory processing with minimal changes in auditory thresholds (Gallun et al., 2012a; Saunders et al., 2015; Bressler et al., 2017). This occurs in age-related or noise-induced sensorineural hearing loss and encompasses putative changes resulting from hair cell or auditory nerve/synapse damage (Hickox and Liberman, 2014; Plack et al., 2014; Bharadwaj et al., 2015; Kujawa and Liberman, 2015; Viana et al., 2015; Liberman, 2017). One consequence could be CAS adaptations in response to peripheral deafferentation (Caspary et al., 2005, 2008; Wang et al., 2009), which has been speculated to impair temporal processing (Walton,

2010; Parthasarathy and Bartlett, 2011, 2012; Rabang et al., 2012). Blast studies on human subjects often used speech and complex temporally modulated stimuli to pin down "hidden" temporal processing losses that were not apparent with simple audiological measures (Gallun et al., 2012b; Saunders et al., 2015; Bressler et al., 2017; Kubli et al., 2018). However, blast studies in animals rarely go beyond simple auditory stimuli such as clicks, tones and AM modulation in a quiet background (Ewert et al., 2012; Race et al., 2017; Masri et al., 2018).

Using the same rat model as our previous publication (Race et al., 2017), our study documents a detailed time course of blast-induced hearing loss recovery in the subcortical CAS using auditory evoked potentials (AEPs). We specifically chose Iterated Rippled Noise (IRN) with pitch sweep alongside Amplitude Modulation (AM) stimuli in quiet and in modulated noise as temporally complex stimuli in assessing the processing of temporal attributes. IRN was used in neurophysiological and behavioral studies in both human (Krishnan et al., 2014, 2015; Peter et al., 2014; Wagner et al., 2017; Shearer et al., 2018) and animal models (Bendor and Wang, 2005; Alsindi et al., 2018), creating "pseudo-pitch" pitch contours with broadband carriers. IRN bypasses limitations posed by animal frequency range as well as permitting easily adjustable pitch intelligibility by altering the number of noise iterations and thus, the strength of temporal regularity and pitch salience (Patterson et al., 1996).

Materials and Methods

Subject

Male Sprague-Dawley rats (3-4 months) were assigned into Sham group and Blast group randomly. A total of 11 Sham animals and 13 blast animals were used in this study. All animals were kept and raised in relatively quiet and standard laboratory animal housing conditions. All protocols were approved by the Purdue Animals Care and Use Committee (PACUC #1111000280).

Blast Exposure

Animals were anesthetized through intraperitoneal injection of a ketamine/xylazine cocktail (80 mg/kg and 10 mg/kg, respectively). The absence of eye-blink and paw-withdrawal reflexes was ensured prior to proceeding. Anesthetized animals were then placed on a platform beneath an open-ended shock tube to be exposed to the blast event, as described in our prior publications (Song et al., 2015; Walls et al., 2016; Race et al., 2017).

For the Blast group, each rat's head was positioned beneath the open end of the shock tube such that the dorsum of the skull was the incident surface exposed to a composite blast (shock wave + blast wind). A custom plexiglass housing was temporarily placed over the animal's torso for body protection to avoid cardiac or pulmonary effects of blast and to simulate the protective effects of military body armor (Rafaels et al., 2011). The head was fixed with a stereotaxic head frame with bite bar and ear bars (Kopf Instruments) to prevent blast wind-induced head acceleration. The blast exposure exhibited a recorded pressure profile with a rise to peak pressure within 0.3 msec,

followed by overpressure and underpressure periods as follows: side-on (static) 150 kPa maximum overpressure, 1.25 msec overpressure duration, and 20 kPa minimum underpressure; face on (dynamic) 160 kPa maximum overpressure, 1.75 msec overpressure duration, and 5 kPa minimum underpressure. These conditions were the same as reported in our prior publications (Song et al., 2015; Walls et al., 2016; Race et al., 2017). All but one blast animal survived the exposure without displaying any external deficit during each animal's longitudinal follow-up period.

Sham animals were placed equidistant from the blast source, but out of the path of the shockwave, therefore only exposed to the blast noise. Tympanic membrane integrity was verified for all Blast and Sham animals after injury using a surgical microscope.

(Insert Fig. 1 about here)

Auditory Evoked Potential Recordings

The animals underwent two-channel Auditory Evoked Potential (AEP) recordings at the following time points: pre-exposure (baseline), 1 day, 4 days, 7 days, 10 days, 14 days, 1 month, and 2 months. While the animals were under 1.8-2% isoflurane anesthesia, subdermal needle electrodes (Ambu) were inserted in the following locations (Fig. 1A): Channel 1 positive electrode was placed along the midline of the head (mid-sagittal) oriented Fz to Cz. Channel 2 positive electrode was positioned C3 to C4 along the interaural line. The negative/inverting electrode (used with positive electrodes for both channels 1 and 2) was placed under the mastoid of the right ear

ipsilateral to the speaker. A ground electrode was placed in the back of the animal. These configurations were consistent with prior publications from our laboratory (Parthasarathy and Bartlett, 2011, 2012; Parthasarathy et al., 2014; Lai and Bartlett, 2015; Lai et al., 2017). Electrode impedances were confirmed to be less than 1 kΩ using a low impedance amplifier (RA4LI, TDT). After electrode placement, we subsequently sedated the animals by intramuscular injection of 0.2-0.3 mg/kg dexmedetomidine (Dexdomitor). AEP recordings were performed 10-15 min after removal from isoflurane to avoid anesthetic effects. The animals could respond to pain and acoustic stimuli but tended sit calmly under dexmedetomidine sedation, allowing about 3 hours of recording time.

Acoustic stimuli were presented free-field to the right ear (90° azimuth) of animals with directly in front of the animals' face as the reference for 0° azimuth, using a calibrated speaker (Bowers and Wilkins) at a distance of 115 cm directly facing the right ear. The measurements used in this study included auditory brainstem responses (ABRs), middle-latency responses (MLRs), envelop-following responses (EFRs) using AM in noise stimuli, and IRNs.

ABR and MLR

6 Sham animals and 10 Blast animals were used in ABR analysis. For ABR, rectangular clicks (0.1 msec duration) and tone-pips (2 msec duration, 0.5 msec $\cos^2$ rise-fall time) with frequencies of 8 kHz and 16kHz were used. 8 kHz and 16 kHz were

chosen based on previous findings: with 6-16 kHz being the most sensitive hearing region of rats, 8 kHz near the most sensitive region of normal rat audiogram (Parthasarathy et al., 2014) and hearing of frequencies higher than 8 kHz being most vulnerable to blast injury (Race et al., 2017). The sound levels of clicks and pips ranged from 90 to 10 dB peak SPL in 5-dB steps. All stimuli were presented in alternating polarity at 26.6 per second with 1500 repetitions (750 at each polarity). A 20 msec acquisition window (0-20 msec) was used.

Data were processed with a 30 Hz high-pass (HP) filter and a 3000 Hz low-pass (LP) filter prior to analysis. The ABR threshold was visually determined as the minimum sound level that produced a distinct ABR waveform, with confirmation from two other researchers. The ABR amplitudes of waves I and V from channel 2 were estimated as the differences of each wave's amplitude, as seen in BioSigRP (TDT) and the baseline amplitude (measured as an average of 2 msec waveform prior to the cochlear microphonic).

6 Sham animals and 8 Blast animals were used in MLR analysis. For MLR, similar rectangular clicks and 8 kHz tone pips of alternating polarity as in ABR were used but were presented at a slower rate (3.33/sec vs. 26.6/sec in ABRs) and with a recording window of longer duration (100 msec vs. 20 msec in ABRs). This time window provides enough time to capture the stimulus-evoked "middle-latency" neural responses from the auditory midbrain, thalamus and cortex (Barth and Shi Di, 1991; McGee et al., 1991; Di and Barth, 1992; McGee and Kraus, 1996; Phillips et al., 2011; Šuta et al., 2011)

alongside ABR. Stimuli were presented at 80 dB sound pressure level (SPL) and 30 dB sensation level (SL, 30 dB above corresponding ABR thresholds), as determined in the previous ABR recordings. 1500 repetitions were collected over an acquisition time window of 100 msec to obtain an average response. Only one animal exhibited hearing threshold higher than 80 dB SPL at only one time point, for which MLR recording has been excluded for that point.

Data were processed with HP (fc = 10 Hz) and LP (fc = 300 Hz) filters prior to analysis.

EFRs

EFRs were recorded during the same recording session following ABRs and MLRs using the same electrode configurations with similar techniques to Lai and Bartlett (2018) and Lai (Lai et al., 2017). The two channels were sensitive to a complementary range of amplitude modulation frequencies (AMFs) (Parthasarathy and Bartlett, 2012), with channel 1 (mid-sagittal) being more sensitive to higher AMFs (90-2048 Hz) while channel 2 (interaural) is more sensitive to lower AMFs (8-90 Hz). The AM stimuli used for EFRs were sinusoidally amplitude-modulated (AM) sounds, with Gaussian noise, 8 kHz tone, or 16 kHz tone as carriers, and under 100% and 50% modulation depth with a stimulus duration of 200 msec. The AMFs selected for this study are 10 Hz, 45 Hz, and 256 Hz, based on the findings in Race at al. (Race et al., 2017), which found significant differences, particularly at the lower AMFs. The acquisition window was 300 msec long, and each response was an average of 200 repetitions. The stimuli were presented at 30 dB SL. For animals that has a hearing threshold above 70 dB SPL,

which usually happens on day 1 post exposure, EFR were not collected at the time point due to the limitation of the speaker and BiosigRP.

For AM in Noise stimuli, the same EFRs were used alongside a 71 Hz sinusoidally AM masker of the same length and onset, with Gaussian noise as the carrier, similar to Lai and Bartlett (Lai and Bartlett, 2018). Noise AM maskers were presented at sound levels of 20dB SNR and 0SNR to the sound level of target AM. Prior to EFR amplitude analysis, data were passed through an LP filter of 3000 Hz and a high-pass filter that was either slightly below the AMF for AMFs <90 Hz, or 80 Hz for AMFs ≥ 90 Hz.

IRNs

For 6 Sham animals and 8 Blast animals, IRNs were recorded during the same recording session following the previous stimuli using the same electrode configurations. Sound level of presentation were 30 dB SL (above click hearing threshold). Data for animals that has a hearing threshold above 70 dB SPL were not collected at the time point.

IRN tone stimuli were created by sequential delay and add operations. Time-varying pitch curves were created by applying polynomial equations to create delays constructed from the fundamental frequencies of Chinese tone 2 and tone 4, delaying Gaussian noise (80 Hz-40 kHz) by the inversion of pitch and adding it back on itself in a recursive manner (Yost, 1996a). The core MATLAB program used for generating

IRN was modified from that used by Krishnan et al. (Krishnan et al., 2014, 2015) This would generate dynamic, curvilinear pitch patterns (Swaminathan et al., 2008) that preserves variations in pitch using a broadband carrier. The number of iteration steps for these stimuli was 32, beyond which there is little or no change in pitch salience (Yost, 1996b).

IRN iteration (ite) stimuli were created with the same polynomial equations used for tone 2, but with changing iterations to create an array of IRN stimuli with different salience of the pitch component. The numbers of iteration steps were 32, 16, 8, 4, and 2.

All IRN stimuli consisted of pairs of waveforms in original and inversed polarities to compensate for envelope or fine structure response under different calculations and to cancel any microphonics. The stimulus duration was 250 msec, and the acquisition window was 300 msec long. Each response was an average of 200 repetitions.

Statistics

Statistics were performed with statistics software JASP (Version 0.11, JASP Team, 2019).

All statistics for ABR and EFR utilized 2-way repeated measures ANOVA test ($\alpha = 0.05$) to check the significance of each main effect and interaction, undergoing Greenhouse-Geisser sphericity corrections (Greenhouse and Geisser, 1959) and Tukey Post Hoc

corrections (Tukey, 1949). For ABR statistics, Wave I (channel 2), III (channel 1) and V (channel 2) were measured at each time point, corresponding to the auditory nerve (Wave I), cochlear nucleus (Wave III), and rostral brainstem/IC sources (Wave V) (Fig. 1B). For EFR statistics, responses were analyzed from channel 2 for 10 Hz and 45 Hz, and from channel 1 for 256 Hz. Prior to statistical tests, EFR amplitudes at signal frequencies were acquired through Fast Fourier Transformation (FFT) in MATLAB (MathWorks) similar to (Lai and Bartlett, 2018).

For MLR statistics, P1, N1, P2, and N2 (Fig. 5A) peaks were measured at each time point, corresponding to subcortical (P1), thalamocortical (N1) and cortical sources (P2, N2). Peak amplitudes were normalized to the pre-blast exposure baseline measurements for display in Fig. 5C, D. The peak amplitudes at each time point were compared to the pre-stimulus baseline using a paired sign-rank test, with a 0.05 significance criterion.

For IRN statistics, we performed moving-window autocorrelations in 25 msec moving windows (5 msec steps) on each response waveform to simulate physiological tracking of temporal periodicity. Peak autocorrelation frequency was defined by the inverse of the time lag where peak autocorrelation value occurs in each window. This process yielded a total of 51 peak frequencies that reflect the frequency representation of the IRN auditory response. Of those, 45 occured during the stimulus. The peak frequencies were then compared to the "pseudopitches" of the IRN stimuli on

corresponding time points. A value within 5 Hz of absolute difference to corresponding "pseudopitch" was considered "tracked." We used this number of "tracked" peak frequencies, or "pitch-tracking score," as a quantification for IRN performance. The significance of each main effect (time, blast condition, and IRN iterations) and interaction was assessed using similar 2-way repeated measures ANOVA test as ABR statistics ($\alpha = 0.05$). For response-to-response correlation (Fig. 8D), the cross-correlation was measured between the response to the IRN stimuli pre-exposure and the response to the same stimulus post-exposure. Blast versus sham group was tested using the paired sign-rank test for this measure ($\alpha = 0.05$).

Results

A. ABR and MLR

ABR Thresholds

(Insert Fig. 2 about here)

Click ABR recordings captured distinctive courses of threshold changes over the two months post-exposure for blast and sham animals (Fig. 2). A large, >30dB SPL maximum threshold increase was observed in post-blast-exposure animals (Fig. 2, red lines). Adjacent animals exposed only to blast noise (sham) did not undergo significant threshold shifts (Fig. 2, blue lines). Thresholds for blast group animals showed clear recovery during the first two weeks, with the largest changes occurring between 4 days – 10 days. Thresholds for blast-exposed animals remained significantly elevated

(worse) than those of sham animals throughout the two months post-exposure that were measured ($F=12.727$, $p=0.003$). Significant main effects of both Group ($F=61.943$, $p=<0.001$, $\eta^2_p=0.816$) and Time Point ($F=41.932$, $p<0.001$, $\eta^2_p=0.750$), as well as a significant Group*Time Point interaction effect ($F=23.503$, $p<0.001$, $\eta^2_p=0.627$), were observed.

Similar trends were observed with tone ABR recordings of 8 kHz and 16 kHz (Fig. 2), with a significant ($p\leq0.001$) >30 dB increase in threshold within 48 hours post-blast-exposure and most prominent recovery between 4 days – 10 days. 8 kHz threshold differences between blast conditions became non-significant ($F=3.151$, $p=0.098$) at 10 days post-blast. At two weeks post-exposure, 16 kHz thresholds remained significantly elevated ($F=16.527$, $p<0.001$), after which point the thresholds for the two chosen tone frequencies were no longer significantly different between blast and sham. Our rmANOVA analysis using Group and Time Points as factors showed significant main effects of Group (8 kHz: $F=10.847$, $p=0.005$, $\eta^2_p=0.437$; 16 kHz: $F=19.697$, $p<0.001$, $\eta^2_p=0.585$), Time (8 kHz: $F=25.837$, $p<0.001$, $\eta^2_p=0.649$; 16 kHz: $F=20.181$, $p<0.001$, $\eta^2_p=0.590$) and Group*Time Point interaction (8 kHz: $F=13.490$, $p<0.001$, $\eta^2_p=0.491$; 16 kHz: $F=15.860$, $p<0.001$, $\eta^2_p=0.531$) for 8 kHz and 16 kHz threshold respectively. These results demonstrate that broadband click thresholds remain significantly elevated over the 60 days measurement window. 8 kHz thresholds largely returned to baseline (Day 30: 8 dB difference, $p=0.118$; day 60: 4 dB difference, $p=0.965$) after two weeks, and 16 kHz thresholds remained significantly elevated compared to pre-

blast baseline according to post hoc analysis (Day 30: 15.5 dB difference, $p<0.001$; day 60: 14.5 dB difference, $p<0.001$), although the difference between blast and sham was not significant at these time points.

ABR Amplitudes

(Insert Fig. 3 about here)

For our ABR and MLR measurements, we used two sound levels: 80 dB SPL was chosen because it is commonly used in auditory evoked potential studies in rat and human studies (Simpson et al., 1985; Alvarado et al., 2012; Race et al., 2017), and it elicits clear ABR responses in all except the most extreme cases of blast-exposure. In order to compensate for changes in threshold induced by blast exposure, we also measured ABR amplitudes at 30 dB SL above threshold (sensation level, or SL). This enabled us to separate changes in ABR amplitudes due to audibility (threshold) versus those due to threshold-independent changes in subcortical auditory signaling. Note that we did not attempt to compare later ABR waves with equivalent wave I amplitudes, as in Lai et al. (2017).

80 dB SPL

ABR wave amplitudes were assessed for wave I (putative auditory nerve), III (putative cochlear nuclei), and V (putative rostral brainstem and inferior colliculus) in response to click stimuli at 80 dB SPL (Fig. 3) and 30 dB SL (Fig. 4). Repeated measures statistics are shown in Table 1. Click, 8 kHz, and 16kHz Wave I amplitudes at 80 dB

SPL all exhibited significant main effect of Group, Time, and Group*Time interaction. Click wave I amplitudes at 80 dB SPL were smaller in blast animals at all time points tested, only becoming non-significant at two months ($F=4.393$, $p=0.055$) despite a 30% difference in mean amplitudes. By contrast, sham animals maintained a consistent click wave 1 amplitude (Fig. 3). Interestingly, the Wave I amplitude difference between groups for both 8 kHz and 16 kHz exhibited two distinct windows: from 1 day to 7 days post-exposure ($p<0.001$), and 14 days post-exposure (8 kHz: $p=0.049$; 16 kHz, $p<0.001$), while on 10 days post-exposure the differences between groups are not significant. Post hoc comparison revealed that both groups experience a second, late-stage (60 days) decrease of Wave I for 8 kHz and 16 kHz ABR, but this decrease is only significant for the blast group (8 kHz: 0.517 μV difference, $p=0.008$; 16 kHz: 0.560 μV difference, $p<0.001$).

For Wave III amplitude at 80 dB SPL, all carrier groups also exhibited significant main effect of Group, Time, and Group*Time. Blast animals experienced a dramatic drop from pre-exposure to day 1, and post hoc analysis revealed that Wave III amplitude is still significantly defected compared to pre-exposure for Click ($T=-4.538$, $p=0.002$) and 16k ($T=-4.678$, $p<0.001$) at 2 months , while 8k amplitude recovered to pre-exposure level on day 60. Though not suffering from the blast impact on day 1, the sham group exhibit an insignificant but consistent decrease in Wave III amplitude on all carrier conditions at 80 dB SPL. Simple main effect analysis showed that differences between groups persists to 30 days for Click ($F=4.714$, $p=0.048$), 10 days for 8k ($F=5.847$,

p=0.030), and 14 days for 16k Hz (F=8.374, p=0.012).

Click Wave V amplitude at 80 dB SPL exhibited a similar trend to Click Wave I, with significant main effect of Group and significant Group*Time interaction effect. But the amplitude difference is not significant from 30 days onward (F=3.651, p=0.077). Similarly, significant main effects of Group, Time and Group*Time interaction can be observed in 8 kHz and 16 kHz ABR Wave V at 80 dB SPL, although between-group difference for 8 kHz is lost at 10 days and onwards (F=2.043, p=0.175), while for 16 kHz it became not significant at 30 days and onwards (F=0.888, p=0.362), similar to Click.

(Insert Fig. 4 about here)

30 dB SL

Because of drastic blast-induced threshold changes over two months, measurements were also made at 30 dB SL. Repeated measures statistics are shown in Table 2. For Wave I, significant main effects of Time but not Group were observed for click, 8 kHz, and 16 kHz. Additionally, significant Group*Time interaction effects were only observed for Click and 16 kHz.

For Wave III, a significant main effect is only observed in Click Group*Time interaction, with the only significant differences between time points observed in Blast day 1 vs. Blast pre-exposure and Blast day 4 vs. blast pre-exposure. No significant difference in

Wave III amplitudes has been observed at any time point between groups or time points in 8k and 16k.

The only significant main effect observed in Wave V at 30 dB SL was the effect of Time in Click, as well as a significant Group*Time interaction effect.

In summary, with the hearing threshold being accounted for, and the simple main effect of Group diminished, ABR wave amplitudes still changed significantly over time post-blast-exposure. The effect of time on Blast and Sham group manifested differently, with Group*Time interactions observed in multiple waves and carriers, but most robustly represented by Click. Wave III and V showed similar trends of diminished differences with pure tone ABRs measured here.

(Insert Fig. 5 about here)

B. MLR

In order to observe thalamocortical and cortical neural transmission in response to acoustic transients, we recorded middle-latency auditory responses to click and 8 kHz tone stimuli. These stimuli were identical to those used for ABR, but the presentation rate was much slower, and the analysis window and filters were different (see Methods). Measurements were made for the first four main peaks of the MLR. Here, P1 corresponds to subcortical activity, largely encompassing the ABR. N1 corresponds to thalamocortical transmission, while P2 and N2 are thought to correspond to primarily

cortical activity (Deiber et al., 1988; Liégeois-Chauvel et al., 1994; Tichko and Skoe, 2017; Musiek and Nagle, 2018).

80 dB SPL responses

In blast animals, all waves were decreased relative to pre-blast baseline for days 1-7 post-blast ($p<0.05$, sign-rank test) in response to 80 dB SPL click stimuli. Grand average traces are shown for MLR responses in this time window in Fig. 5A, relative to the pre-blast waveform (thick blue line in A-D). Even after the blast, the morphology and timing of the MLR waveform remained relatively intact, but the amplitudes were significantly diminished. In Fig. 5E-H, wave amplitudes were normalized to the pre-blast waves and measured. Between 7 and 10 days, the early P1 wave recovers to within 10-15% of its baseline amplitude, whereas the later waves recovered more slowly (Fig. 5E). In particular, the N1 wave, thought to reflect thalamocortical transmission (Barth and Shi Di, 1991; McGee et al., 1991, 1992; Di and Barth, 1992; Brett et al., 1996; McGee and Kraus, 1996; Phillips et al., 2011; Šuta et al., 2011), remained significantly lower in blast animals even 60 days post-blast ($p<0.05$, sign-rank test, Fig. 5E). By contrast, the MLR waves in sham animals were largely stable across the measurement time (Fig. 5F). Although there was some decline in the later waves for the last time window, this was not statistically significant (Fig. 5B, D, F).

MLR responses to 8 kHz, 80 dB SPL tone pips largely mirrored the results to clicks, with significant decreases for all waves for post-blast days 1-7 and a lasting decline in

N1 for the duration of measurements ($p<0.05$, sign-rank test, traces not shown). Sham responses did not show any significant changes in MLR waves in response to the 80 dB SPL tone pips.

30 dB SL

MLR responses to clicks at 30 dB SL were reduced in Blast animals 1 day after the blast but recovered to baseline levels afterward. There was a tendency towards elevated P1 amplitudes, but this was not significant (Fig. 5G). Sham animals did not show any significant changes, though there was a tendency towards an increase in wave amplitude (Fig. 5H). Similar results were found for responses to tones at 30 dB SL (not shown).

C. EFR and EFR in noise

Three sets of EFRs were recorded using Gaussian broadband noise (NAM), 8 kHz, and 16 kHz sinusoidal tone carriers correspondingly. Three representative AMFs (10, 45, and 256 Hz) were selected from previous publications (Parthasarathy et al., 2010, 2014; Parthasarathy and Bartlett, 2011, 2012; Race et al., 2017) tested in quiet at 100% and 50% modulation depth. AM stimuli were also presented at 30 dB SL alongside a 71 Hz sinusoidally AM masker of the same length and onset, with Gaussian noise as the carrier, under three noise conditions: no noise, at 20dB SNR and 0 SNR relative to the sound level of target AM. For each carrier, simple main effects of all conditions were analyzed.

(Insert Fig. 6 about here)

Overall, the only significant measurement affected in the Blast group was NAM FFT amplitude ($F=9.629$, $p=0.0018$, $\eta^2_p=0.426$), with 45 Hz being the most affected. Interestingly, in contrast to the lower FFT Amplitude found in Blast AM at 80 dB SPL (Race et al., 2017), when the hearing threshold has been compensated, FFT amplitude of 45 Hz NAM is higher in Blast than in Sham animals. This difference is most salient on day 7 for 45 Hz NAM ($p=0.006$). For 8 kHz SAM and 16 kHz SAM, the slight elevation of AM FFT Amplitude in Blast animals was not significant.

Surprisingly, time did not have a significant interaction across repeated measures for AM response with any carrier either. Not surprisingly, Noise level and Modulation Depth both had a significant repeated measures effect on NAM (Noise level: $F=263.217$, $p<0.001$, $\eta^2_p=0.953$; Depth: $F=455.655$, $p<0.001$, $\eta^2_p=0.972$), 8 kHz SAM (Noise level: $F=19.308$, $p<0.001$, $\eta^2_p=0.580$; Depth: $F=72.031$, $p<0.001$, $\eta^2_p=0.837$) and 16 kHz SAM (Noise level: $F=16.691$, $p<0.001$, $\eta^2_p=0.544$; Depth: $F=49.742$, $p<0.001$, $\eta^2_p=0.780$). Noise level and Depth also have a significant interaction effect with Blast Groups for NAM (Noise level: $F=10.295$, $p<0.001$, $\eta^2_p=0.442$; Depth: $F=6.057$, $p=0.029$, $\eta^2_p=0.318$), meaning these two conditions affect Blast-exposed animals and Sham-only animals differently. Noise level also affects 8 kHz SAM differently between Groups ($F=5.696$, $p=0.008$, $\eta^2_p=0.289$). These conditions do not have significant interaction effects with Blast Group on 16 kHz SAM.

(Insert Fig. 7 about here)

Considering that slow AM (<50 Hz) and faster AM (>50 Hz) are differentially represented throughout cortical and subcortical auditory nuclei (Joris et al., 2004; Wang et al., 2008), we considered the effects of Blast and Sham conditions between different modulation frequencies. For NAM, the only significant interaction effects between Group and other modifiers were observed under 45 Hz modulation frequency. Noise level had significant interaction effects with both Blast Group ($F=6.130$, $p=0.011$, $\eta^2_p=0.320$) and Depth ($F=19.438$, $p<0.001$, $\eta^2_p=0.599$), while the effect of Time or Depth between Groups is not significantly different for any modulation frequency.

For 8 kHz SAM, the effects of Noise level were applied differently between Blast Groups, as significant interaction effects were observed between Noise and Group for 10 Hz ($F=12.795$, $p=0.001$, $\eta^2_p=0.477$) and 45 Hz ($F=4.878$, $p=0.015$, $\eta^2_p=0.258$) modulation frequencies, though not for 256 Hz. Modulation Depth affects FFT amplitude without regard to blast condition, with no significant interaction effects with Group observed. For 16 kHz SAM, none of the parameters tested has significantly different effects between Groups at 30 dB SL (not shown).

After normalization to each animal's baseline (pre-exposure, quiet and 100% depth) FFT amplitude, the interaction effect between Group and Noise masker is no longer significant for NAM (not shown), but remains strong in 8 kHz SAM at 10 Hz ($F=6.626$,

p=0.018, η^2_p =0.321) and 45 Hz (F=6.882, p=0.008, η^2_p =0.330), with Blast animals showing lower FFT amplitudes at 10Hz, but higher amplitudes at 45Hz. Group showed no significant interaction effects with individual factors otherwise in 16 kHz SAM.

D. IRN

Here, we used time-varying IRN to elicit frequency-following response (FFR) mimicking Mandarin tone 2 (T2, rising) and tone 4 (T4, falling) pitch contours to measure pitch-tracking ability using a broadband speech-like carrier, similar to what has been measured in human studies of auditory learning and hearing loss (Anderson et al., 2010, 2013; Skoe and Kraus, 2010). We used autocorrelation interval contours that simulated pitches similar to the forms of rising (T2) and falling (T4) pitch contours of the Mandarin Chinese vowel /yi/ (Krishnan et al., 2014, 2015, 2017a, 2017b). IRN responses were evaluated based on the pitch-tracking score, which measures the number of windows where the dominant autocorrelation frequency of the response matches that of the IRN stimulus autocorrelation frequency (see Methods). In general, we observed a loss of pitch-tracking fidelity in Blast animals over the two months post-exposure. Even for the most salient pitch (32 Iterations), blast exposure had a significant Group effect on pitch-tracking scores in both Tone 2 (F=6.495, p=0.026, η^2_p=0.351) and Tone 4 (F=6.115, p=0.029, η^2_p=0.338), with the largest mean differences on day 7-10. The interaction effect between Time and Group was not significant.

Blast exposure significantly changed the morphology of the neural response to IRN at

30 dB SL (p=0.016, paired sign-rank test, Fig. 8D), such that the cross-correlation between the pre-exposure response and the post-exposure response was much lower in the Blast group up to 30 days post-blast.

(Insert Fig. 8 about here)

As expected, reduced salience, controlled by reducing iteration number, affected pitch-tracking performances in animals ($F=41.697$, $p<0.001$, $\eta^2_p=0.777$), also showing a significant interaction effect with Time post-exposure ($F=1.722$, $p=0.031$, $\eta^2_p=0.125$). Specifically, pitch-tracking performances to 32 iterations and 16 iterations were the most impacted at 7-10 days post-exposure, with various degrees of recovery over later days. The trend of reduced tracking with reduced salience was not significantly different between Blast group and Sham group. No significant interaction effects with Group was observed for both Time and Iterations (Fig 9).

(Insert Fig. 9 about here)

Discussion

The purpose of this study was to examine the time course of recovery from a single mild blast injury using simple and complex auditory stimuli longitudinally over a two-month period. Our study demonstrated drastic changes in high-frequency and click hearing thresholds from ABR recordings and reductions in putative subcortical and thalamocortical transmission from ABR and MLR recordings throughout the first two weeks post exposure, with scattered persistency at 30 days. Furthermore, the initial

large deficits in neural representations of temporally modulated auditory stimuli recovered to near pre-blast baselines in some cases. The 7-14 day window was particularly rapid in the recovery of many auditory parameters, suggesting this as an research and therapeutic time period.

ABR

We documented the rapid increase of threshold and slow recovery after trauma from blast-exposure. Most notably, a >30 dB increase in threshold was observed for click, 8 kHz, and 16 kHz (Fig. 2). This is consistent with the description of IHC and OHC disturbances across a wide range of frequencies as a result of blast overpressure as stated in multiple previous publications (Patterson and Hamernik, 1997; Ewert et al., 2012; Race et al., 2017). Cho et al. (2013b) reported that ABRs exhibit the least recovery at the highest and lowest frequencies. In the current study, the click stimuli, which have a broad spectrum extending into higher frequencies, were more affected in Blast animals than lower frequency tones (Fig. 2). This broadband threshold shift extended to the last time point at 60 days, though the ~10 dB difference would not be considered clinically relevant.

Over the two-month observation, rapid improvements in ABR threshold and wave amplitudes were observed in the 7-10 days recovery period for waves I, wave III, and wave V. Such rapid recovery could be explained by neuroplastic remodeling within central auditory ABR generator regions (Mulders and Robertson, 2009, 2011, 2013; Mulders et al., 2011; Manzoor et al., 2013; Robertson et al., 2013). Notably, wave V

amplitude recovered earlier than wave I, possibly indicating the role of compensation in auditory midbrain as one of the post-blast recovery mechanisms.

We hypothesized that the recovery of ABR threshold and wave I amplitude were the results of a two-fold process. These parameters showed two waves of post-blast changes: one between 1-10 days post-exposure, and one 10-30 days, as evidenced by Figs. 2 and 3. We hypothesize that these two waves of deficits indicated the distinction of primary, physical impacts to multiple loci in PAS and CAS (Garman et al., 2011; Ewert et al., 2012; Cho et al., 2013b; Song et al., 2015; Walls et al., 2016) and a series of secondary, biochemical impacts surrounding CAS (Laplaca et al., 1997; Knudsen and Øen, 2003; Hamann et al., 2008; Garman et al., 2011; Säljö et al., 2011; Luo et al., 2014a, 2014b; Song et al., 2015; Walls et al., 2016). These two waves of impacts, including cellular membrane damage, oxidative stress, and excitatory/inhibitory changes in auditory midbrain, are all potential contributors to blast-induced subcortical CAS impairments and establish themselves in auditory pathophysiology at different time points after a single blast exposure. Our observation of this two-fold process in blast injury development may prove valuable in determining the critical intervention time windows for various diagnostic and treatment practices. Persistent changes in central auditory circuits may be compounded by the observed persistent increase in high-frequency thresholds, contributing to degraded speech perception (Holmes and Griffiths, 2019; Yeend et al., 2019).

MLR

At 80 dB SPL, we found persistent deficits in thalamocortical and cortical transmission based on the N1, P2 and N2 peaks (Fig. 5A vs. B, C vs. D), which were affected at 30 or 60 days, even after the early P1 response had fully recovered (Fig 5E). These deficits were not present at 30 dB SL, suggesting that effects were at least in part due to shifts in auditory thresholds (Fig. 5G), but the moderate, subclinical threshold shifts observed are probably highly relevant functionally. In veterans and in the general population with lifetime noise exposure, MLR responses were shown to be smaller even when subjects had clinically normal audiograms, and there was some evidence of increased cortical gain (Valderrama et al., 2018; Bramhall et al., 2020). In another study with blast-exposed veterans, most of the changes in auditory-evoked potentials were correlated with hearing loss (Meehan et al., 2019). Together, these results suggest that hearing loss may be the main contributor to MLR changes leading to declines in suprathreshold responses. However, more work needs to be done to examine the relationships between early evoked potentials and later potentials for sustained sounds post-blast, since studies in aging and noise exposure have suggested enhanced cortical responses (Syka and Rybalko, 2000; Sun et al., 2012; Bidelman et al., 2014; Herrmann et al., 2019). These results also suggest that there may be more pronounced hearing deficits from intense combined auditory and mechanical trauma such as blast, compared to medium to intense level of auditory exposure alone, such as recreational or occupational noise (Fulbright et al., 2017; Grinn et al., 2017; Guest et al., 2018).

Amplitude Modulation EFRs

The current study extended an earlier study (Race et al., 2017) to include EFR responses to more challenging auditory stimuli, including lower modulation depth (Fig 6) and in the presence of modulated noise (Fig 7). The Race et al. (2017) study revealed differences in AM processing at 80 dB SPL between blast and sham animals, such that blast animals had lower AM FFR amplitudes, especially at lower modulation frequencies in the 20-50 Hz range. However, when the hearing threshold has been compensated, the differences in AM FFR amplitude diminished and even changed sign (Fig. 6), suggesting that both changes in audibility and changes in the gain of subcortical auditory system are critical contributors to AM FFR deficits in the blast-exposed auditory system. There are complicated interactions between the AM FFR amplitudes, blast exposure, and the presence of noise, evident as a persistent Group*Noise Level interaction effect in both NAM and 8 kHz SAM. AM responses consist of contributions from multiple generators along the auditory neuroaxis, with cortical generators contributing mainly to lower AMFs <50 Hz, and higher frequency AM responses limited to nuclei lower in the auditory neuroaxis. The lack of blast-induced differences at higher AMFs both in the previous study and this study supports the notion that central alterations specific to blast injury and not purely from peripheral blast noise trauma are likely present. Moreover, this distinguishes the blast induced damage from age-related changes, which are most prominent at higher modulation frequencies (Parthasarathy et al. 2010, Parthasarathy and Bartlett 2012, Lai et al.

2017).

The differences in low-middle AMFs were manifested in opposed directions under slow (10 Hz) and middle (45 Hz) AMFs: notably, normalized FFT amplitudes of 8 kHz SAM in noise is lower for blast at 10 Hz modulation frequency, but higher for blast at 45 Hz (Fig 7D). In studies on age-related AN deficit models and AM-in-noise responses in aged animals, decreased sensitivities to lower SNRs in AM-in-noise in damaged auditory systems have been observed (Parthasarathy et al., 2016; Lai et al., 2017; Lai and Bartlett, 2018). This phenomenon could partly explain the changes seen in 45 Hz AMF. It should be noted that the variance in AM responses post-blast exposure could also be a result of post-blast increases in spontaneous activity for DCN and IC units sensitive to tone versus noise carriers (Luo et al., 2014a, 2014b), which could either desynchronize responses or strengthen AM response simply by heightened excitability.

Taken together, our results suggested that: 1) CAS neuroplasticity partially compensates for central deficit after blast exposure; and 2) more challenging stimuli, such as increased complexity and the presence of noise, were more sensitive in revealing subclinical (asymptomatic/non-perceived) CAS dysfunction caused by mild blast exposure than threshold shifts.

IRN EFRs

Bressler et al. (2017) have noted that perceptual and behavioral deficits persist in blast-exposed veterans in the absence of major threshold or ABR abnormalities. Simple auditory tests such as ABRs and AM EFRs in a quiet background are limited indicators of auditory challenges that blast-exposed individuals would face in daily life. The present study investigated how noise affects responses post-blast as well as using IRN stimuli that simulate the pitch trajectories and sound like simple speech sounds. These stimuli may capture the more complex hearing deficits reported by humans who have experienced blast injuries (Gallun et al., 2012a; Saunders et al., 2015; Kubli et al., 2018). IRN may prove to be a valuable diagnostic tool, as it is a broadband stimulus carrying complex temporal information and whose salience can be reliably controlled. We found out that even when click ABR thresholds have returned to subclinical threshold shifts, the deficits in pitch-tracking response to IRN tone stimuli, especially Tone 2 (rising), lingered at 30 days post exposure (Figs. 8D).

Decreased salience (fewer iterations), showed an overall reduction in pitch tracking in Blast animals (Fig. 9), but they were not differentially affected by the number of iterations. It is worth noting that a previous study showed that increased IRN iterations improved auditory stream segregation in normal hearing veterans more than hearing-impaired veterans (Shearer et al., 2018). Although the findings from blast IRN recordings were promising, our result calls for more continuing to probe the main factors influencing physiological and behavioral measures of complex listening to understand the lasting difficulties with noisy speech and speech-like stimuli seen in blast-exposed veterans.

Limitations and Future Directions

This study has examined injuries elicited by a single blast exposure from one specific direction with head fixture and body shielding that did not result in ruptures of the tympanic membrane. Therefore, the deficits observed may be as drastic as that documented by many previous studies in which the injuries were caused by more intense or multiple exposures (Cho et al., 2013b; Du et al., 2013; Luo et al., 2014a, 2014b; Mahmood et al., 2014), often resulting in death or tympanic membrane rupture. The distribution of injuries, neural networks impairment, and potential mechanisms would also differ from models in which blast exposure comes from different orientations, as predicted by pressure wave transmission and strain propagation in animals (Chavko et al., 2011; Dal Cengio Leonardi et al., 2012; Hua et al., 2017) and computational studies (Unnikrishnan et al., 2019). Our model utilized a top-down mild blast model as described by Song et al. (2015) which exerts a blast impact from the top of the skull. The overpressure blast wave passes through the entire rat brain, such that TBI can be observed throughout the brain, including the frontal cortex and in multiple thalamic regions (Walls et al. 2016), and it results in increased ventral BBB membrane permeation and inflammation, encompassing many subcortical auditory nuclei and axonal tracts. While overlapping loci of vulnerability were described in anatomical studies of animal exposed to blast impacts of different or unknown orientations (Knudsen and Øen, 2003; Säljö et al., 2011; Mao et al., 2012b), injury mechanisms of different loci and nature may be expected from blast impacts from a different angle.

Moreover, non-invasive physiological measurements of the auditory thalamus and cortex may be indicators of more widespread blast damage in auditory and non-auditory brain regions.

Conclusion

Based on our chronic longitudinal AEP measurements over a two-month period, this study documented the significant changes in auditory pathophysiology and a potential multi-stage recovery process in animals exposed to a single mild blast trauma. We found that challenging, broadband conditions such as the presence of a noise masker in AM stimuli, as well as IRN stimuli, can better elucidate mild blast-induced auditory deficit during the 7-14-day period.

Acknowledgments

The authors would like to thank Jonathan Tang, Brandon Coventry, Alex Sommers, Nanami Miyazaki, and all the other members in Central Auditory Processing Lab and Lab of Translational Neuroscience for their generous assistance in the completion of this study.

Author contributions

Study concept and design: Edward Bartlett, Riyi Shi, Emily X. Han, Joseph M. Fernandez.

Animal Blast Exposure: Joseph M. Fernandez.

Electrophysiology: Emily X. Han, Caitlin Swanberg.

Data analysis and interpretation: Emily X. Han, Edward Bartlett, Joseph M. Fernandez.

Writing of the manuscript: Emily X. Han, Edward Bartlett.

Critical revision of the manuscript: Riyi Shi, Joseph M. Fernandez, Caitlin Swanberg.

Study supervision and obtainment of funding: Edward Bartlett, Riyi Shi.

Funding

This study is funded by Indiana CTSI 11917.

Disclosures

Riyi Shi is a co-founder of Neuro Vigor, a company developing novel drug treatments and diagnostic approaches for neurodegenerative diseases and neurotrauma.

References

Alsindi S, Patterson RD, Sayles M, Winter IM (2018) The responses of single units to simple and complex sounds from the superior olivary complex of the Guinea pig. In: Acta Acustica united with Acustica, pp 856–859. S. Hirzel Verlag GmbH.

Alvarado JC, Fuentes-Santamaría V, Jareño-Flores T, Blanco JL, Juiz JM (2012) Normal variations in the morphology of auditory brainstem response (ABR) waveforms: A study in wistar rats. Neurosci Res 73:302–311.

Anderson S, Parbery-Clark A, White-Schwoch T, Kraus N (2013) Auditory brainstem response to complex sounds predicts self-reported speech-in-noise performance. J Speech, Lang Hear Res 56:31–43.

Anderson S, Skoe E, Chandrasekaran B, Kraus N (2010) Neural timing is linked to speech perception in noise. J Neurosci 30:4922–4926.

Armstrong RC, Mierzwa AJ, Marion CM, Sullivan GM (2016) White matter involvement after TBI: Clues to axon and myelin repair capacity. Exp Neurol 275 Pt 3:328–333.

Barth DS, Shi Di (1991) The functional anatomy of middle latency auditory evoked potentials. Brain Res 565:109–115.

Bendor D, Wang X (2005) The neuronal representation of pitch in primate auditory cortex. Nature 436:1161–1165.

Berger G, Finkelstein Y, Avraham S, Himmelfarb M (1997) Patterns of hearing loss in non-explosive blast injury of the ear. J Laryngol Otol 111:1137–1141.

Bharadwaj HM, Masud S, Mehraei G, Verhulst S, Shinn-Cunningham BG (2015)

Individual differences reveal correlates of hidden hearing deficits. J Neurosci 35:2161–2172.

Bidelman GM, Villafuerte JW, Moreno S, Alain C (2014) Age-related changes in the subcortical-cortical encoding and categorical perception of speech. Neurobiol Aging 35:2526–2540.

Bramhall NF, Niemczak CE, Kampel SD, Billings CJ, McMillan GP (2020) Evoked Potentials Reveal Noise Exposure–Related Central Auditory Changes Despite Normal Audiograms. Am J Audiol 29:152–164.

Bressler S, Goldberg H, Shinn-Cunningham B (2017) Sensory coding and cognitive processing of sound in Veterans with blast exposure. Hear Res 349:98–110.

Brett B, Krishnan G, Barth DS (1996) The effects of subcortical lesions on evoked potentials and spontaneous high frequency (gamma-band) oscillating potentials in rat auditory cortex. Brain Res 721:155–166.

Caspary DM, Ling L, Turner JG, Hughes LF (2008) Inhibitory neurotransmission, plasticity and aging in the mammalian central auditory system. J Exp Biol 211:1781–1791.

Caspary DM, Schatteman T a, Hughes LF (2005) Age-related changes in the inhibitory response properties of dorsal cochlear nucleus output neurons: role of inhibitory inputs. J Neurosci 25:10952–10959.

Cave K, Cornish EM, Chandler DW (2007) Blast Injury of the Ear: Clinical Update from the Global War on Terror. Mil Med 172:726–730.

Chavko M, Watanabe T, Adeeb S, Lankasky J, Ahlers ST, McCarron RM (2011)

Relationship between orientation to a blast and pressure wave propagation inside the rat brain. J Neurosci Methods 195:61–66.

Cho HJ, Sajja VSSS, VandeVord PJ, Lee YW (2013a) Blast induces oxidative stress, inflammation, neuronal loss and subsequent short-term memory impairment in rats. Neuroscience 253:9–20.

Cho S II, Gao SS, Xia A, Wang R, Salles FT, Raphael PD, Abaya H, Wachtel J, Baek J, Jacobs D, Rasband MN, Oghalai JS (2013b) Mechanisms of Hearing Loss after Blast Injury to the Ear. PLoS One 8.

Cloots RJH, van Dommelen JAW, Nyberg T, Kleiven S, Geers MGD (2011) Micromechanics of diffuse axonal injury: influence of axonal orientation and anisotropy. Biomech Model Mechanobiol 10:413–422.

Cohen JT, Ziv G, Bloom J, Zikk D, Rapoport Y, Himmelfarb MZ (2002) Blast injury of the ear in a confined space explosion: Auditory and vestibular evaluation. Isr Med Assoc J 4:559–562.

Dal Cengio Leonardi A, Keane NJ, Bir CA, Ryan AG, Xu L, VandeVord PJ (2012) Head orientation affects the intracranial pressure response resulting from shock wave loading in the rat. J Biomech 45:2595–2602.

Deiber MP, Ibañez V, Fischer C, Perrin F, Mauguière F (1988) Sequential mapping favours the hypothesis of distinct generators for Na and Pa middle latency auditory evoked potentials. Electroencephalogr Clin Neurophysiol Evoked Potentials 71:187–197.

DePalma RG, Burris DG, Champion HR, Hodgson MJ (2005) Current concepts: Blast

injuries. N Engl J Med 352:1335–1342.

Di S, Barth DS (1992) The functional anatomy of middle-latency auditory evoked potentials: Thalamocortical connections. J Neurophysiol 68:425–431.

Du X, Ewert DL, Cheng W, West MB, Lu J, Li W, Floyd RA, Kopke RD (2013) Effects of antioxidant treatment on blast-induced brain injury Holvoet P, ed. PLoS One 8:e80138.

Ewert DL, Lu J, Li W, Du X, Floyd R, Kopke R (2012) Antioxidant treatment reduces blast-induced cochlear damage and hearing loss. Hear Res 285:29–39.

Frati A, Cerretani D, Fiaschi AI, Frati P, Gatto V, La Russa R, Pesce A, Pinchi E, Santurro A, Fraschetti F, Fineschi V (2017) Diffuse Axonal Injury and Oxidative Stress: A Comprehensive Review. Int J Mol Sci 18.

Fulbright ANC, Le Prell CG, Griffiths SK, Lobarinas E (2017) Effects of Recreational Noise on Threshold and Suprathreshold Measures of Auditory Function. Semin Hear 38:298–318.

Gallun FJ, Diedesch AC, Kubli LR, Walden TC, Folmer RL, Samantha Lewis S, McDermott DJ, Fausti SA, Leek MR (2012a) Performance on tests of central auditory processing by individuals exposed to high-intensity blasts. J Rehabil Res Dev 49:1005–1024.

Gallun FJ, Lewis MS, Folmer RL, Diedesch AC, Aud ;, Kubli LR, McDermott DJ, Walden TC, Fausti S a, Lew HL, Leek MR (2012b) Implications of blast exposure for central auditory function: a review. J Rehabil Res Dev 49:1059–1074.

Garman RH, Jenkins LW, Switzer RC, Bauman RA, Tong LC, Swauger P V., Parks SA, Ritzel D V., Dixon CE, Clark RSB, Bayır H, Kagan V, Jackson EK, Kochanek PM (2011) Blast Exposure in Rats with Body Shielding Is Characterized Primarily by Diffuse Axonal Injury. J Neurotrauma 28:947–959.

Greenhouse SW, Geisser S (1959) On methods in the analysis of profile data. Psychometrika 24:95–112.

Grinn SK, Wiseman KB, Baker JA, Le Prell CG (2017) Hidden hearing loss? No effect of common recreational noise exposure on cochlear nerve response amplitude in humans. Front Neurosci 11:465.

Guest H, Munro KJ, Prendergast G, Millman RE, Plack CJ (2018) Impaired speech perception in noise with a normal audiogram: No evidence for cochlear synaptopathy and no relation to lifetime noise exposure. Hear Res 364:142–151.

Hamann K, Durkes A, Ouyang H, Uchida K, Pond A, Shi R (2008) Critical role of acrolein in secondary injury following ex vivo spinal cord trauma. J Neurochem 107:712–721.

Herrmann B, Buckland C, Johnsrude IS (2019) Neural signatures of temporal regularity processing in sounds differ between younger and older adults. Neurobiol Aging 83:73–85.

Hickox AE, Liberman MC (2014) Is noise-induced cochlear neuropathy key to the generation of hyperacusis or tinnitus? J Neurophysiol 111:552–564 Available at: http://www.ncbi.nlm.nih.gov/pubmed/24198321 [Accessed January 8, 2019].

Holmes E, Griffiths TD (2019) ‘Normal’ hearing thresholds and fundamental auditory grouping processes predict difficulties with speech-in-noise perception. Sci Rep 9:1–11.

Hua Y, Wang Y, Gu L (2017) Primary blast waves induced brain dynamics influenced by head orientations. Biomed Eng Lett 7:253–259.

Johnson VE, Stewart W, Smith DH (2013) Axonal pathology in traumatic brain injury. Exp Neurol 246:35–43.

Joris PX, Schreiner CE, Rees A (2004) Neural Processing of Amplitude-Modulated Sounds. American Physiological Society.

Kerr AG (1980) The effects of blast on the ear. J Laryngol Otol 94:107–110.

Knudsen SK, Øen EO (2003) Blast-induced neurotrauma in whales. Neurosci Res 46:377–386.

Krishnan A, Gandour JT, Suresh CH (2014) Cortical pitch response components show differential sensitivity to native and nonnative pitch contours. Brain Lang 138:51–60.

Krishnan A, Gandour JT, Suresh CH (2015) Pitch processing of dynamic lexical tones in the auditory cortex is influenced by sensory and extrasensory processes. Eur J Neurosci 41:1496–1504.

Krishnan A, Gandour JT, Xu Y, Suresh CH (2017a) Language-dependent changes in pitch-relevant neural activity in the auditory cortex reflect differential weighting of temporal attributes of pitch contours. J Neurolinguistics 41:38–49.

Krishnan A, Suresh CH, Gandour JT (2017b) Changes in pitch height elicit both

language-universal and language-dependent changes in neural representation of pitch in the brainstem and auditory cortex. Neuroscience 346:52–63.

Kubli LR, Brungart D, Northern J (2018) Effect of Blast Injury on Auditory Localization in Military Service Members. Ear Hear 39:457–469.

Kujawa SG, Liberman MC (2015) Synaptopathy in the noise-exposed and aging cochlea: Primary neural degeneration in acquired sensorineural hearing loss. Hear Res 330:191–199.

Lai J, Bartlett EL (2015) Age-related shifts in distortion product otoacoustic emissions peak-ratios and amplitude modulation spectra. Hear Res 327:186–198.

Lai J, Bartlett EL (2018) Masking Differentially Affects Envelope-following Responses in Young and Aged Animals. Neuroscience 386:150–165.

Lai J, Sommer AL, Bartlett EL (2017) Age-related changes in envelope-following responses at equalized peripheral or central activation. Neurobiol Aging 58:191–200.

Laplaca MC, Lee VMY, Thibault LE (1997) An in vitro model of traumatic neuronal injury: Loading rate-dependent changes in acute cytosolic calcium and lactate dehydrogenase release. J Neurotrauma 14:355–368.

Leung LY, VandeVord PJ, Dal Cengio AL, Bir C, Yang KH, King AI (2008) Blast related neurotrauma: A review of cellular injury. MCB Mol Cell Biomech 5:155–168.

Lew HL, Garvert DW, Pogoda TK, Hsu P Te, Devine JM, White DK, Myers PJ, Goodrich GL (2009) Auditory and visual impairments in patients with blast-

related traumatic brain injury: Effect of dual sensory impairment on functional independence measure. J Rehabil Res Dev 46:819–826.

Liberman MC (2017) Noise-induced and age-related hearing loss: New perspectives and potential therapies. F1000Research 6:1–11.

Liégeois-Chauvel C, Musolino A, Badier JM, Marquis P, Chauvel P (1994) Evoked potentials recorded from the auditory cortex in man: evaluation and topography of the middle latency components. Electroencephalogr Clin Neurophysiol Evoked Potentials 92:204–214.

Luo H, Pace E, Zhang X, Zhang J (2014a) Blast-Induced tinnitus and spontaneous firing changes in the rat dorsal cochlear nucleus. J Neurosci Res 92:1466–1477.

Luo H, Pace E, Zhang X, Zhang J (2014b) Blast-induced tinnitus and spontaneous activity changes in the rat inferior colliculus. Neurosci Lett 580:47–51.

Mahmood G, Mei Z, Hojjat H, Pace E, Kallakuri S, Zhang JS (2014) Therapeutic effect of sildenafil on blast-induced tinnitus and auditory impairment. Neuroscience 269:367–382.

Manzoor NF, Gao Y, Licari F, Kaltenbach JA (2013) Comparison and contrast of noise-induced hyperactivity in the dorsal cochlear nucleus and inferior colliculus. Hear Res 295:114–123.

Mao JC, Pace E, Pierozynski P, Kou Z, Shen Y, Vandevord P, Haacke EM, Zhang X, Zhang J (2012a) Blast-induced tinnitus and hearing loss in rats: Behavioral and imaging assays. J Neurotrauma 29:430–444.

Mao JC, Pace E, Pierozynski P, Kou Z, Shen Y, VandeVord P, Haacke EM, Zhang X,

Zhang J (2012b) Blast-Induced Tinnitus and Hearing Loss in Rats: Behavioral and Imaging Assays. J Neurotrauma 29:430–444.

Masri S, Zhang LS, Luo H, Pace E, Zhang J, Bao S (2018) Blast Exposure Disrupts the Tonotopic Frequency Map in the Primary Auditory Cortex. Neuroscience 379:428–434.

McGee T, Kraus N (1996) Auditory development reflected by middle latency response. Ear Hear 17:419–429.

McGee T, Kraus N, Comperatore C, Nicol T (1991) Subcortical and cortical components of the MLR generating system. Brain Res 544:211–220.

McGee T, Kraus N, Littman T, Nicol T (1992) Contributions of medial geniculate body subdivisions to the middle latency response. Hear Res 61:147–154.

Meehan A, Hebert D, Deru K, Weaver LK (2019) Longitudinal study of hyperbaric oxygen intervention on balance and affective symptoms in military service members with persistent post-concussive symptoms. J Vestib Res Equilib Orientat 29:205–219.

Mulders WHAM, Ding D, Salvi R, Robertson D (2011) Relationship between auditory thresholds, central spontaneous activity, and hair cell loss after acoustic trauma. J Comp Neurol 519:2637–2647.

Mulders WHAM, Robertson D (2009) Hyperactivity in the auditory midbrain after acoustic trauma: dependence on cochlear activity. Neuroscience 164:733–746.

Mulders WHAM, Robertson D (2011) Progressive centralization of midbrain hyperactivity after acoustic trauma. Neuroscience 192:753–760.

Mulders WHAM, Robertson D (2013) Development of hyperactivity after acoustic trauma in the guinea pig inferior colliculus. Hear Res 298:104–108.

Musiek F, Nagle S (2018) The middle latency response: A review of findings in various central nervous system lesions. J Am Acad Audiol 29:855–867.

Parthasarathy A, Bartlett E (2012) Two-channel recording of auditory-evoked potentials to detect age-related deficits in temporal processing. Hear Res 289:52–62.

Parthasarathy A, Bartlett EL (2011) Age-related auditory deficits in temporal processing in F-344 rats. Neuroscience 192:619–630.

Parthasarathy A, Cunningham PA, Bartlett EL (2010) Age-related differences in auditory processing as assessed by amplitude-modulation following responses in quiet and in noise. Front Aging Neurosci 2:152.

Parthasarathy A, Datta J, Torres JAL, Hopkins C, Bartlett EL (2014) Age-related changes in the relationship between auditory brainstem responses and envelope-following responses. JARO - J Assoc Res Otolaryngol 15:649–661.

Parthasarathy A, Lai J, Bartlett EL (2016) Age-Related Changes in Processing Simultaneous Amplitude Modulated Sounds Assessed Using Envelope Following Responses. JARO - J Assoc Res Otolaryngol 17:119–132.

Patterson JH, Hamernik RP (1997) Blast overpressure induced structural and functional changes in the auditory system.

Patterson RD, Handel S, Yost WA, Jaysurya Datta A (1996) The relative strength of the tone and noise components in iterated rippled noise. J Acoust Soc Am

100:3286–3294.

Peter V, Wong K, Narne VK, Sharma M, Purdy SC, McMahon C (2014) Assessing spectral and temporal processing in children and adults using Temporal Modulation Transfer Function (TMTF), Iterated Ripple Noise (IRN) perception, and Spectral Ripple Discrimination (SRD). J Am Acad Audiol 25:210–218.

Phillips DJ, Schei JL, Meighan PC, Rector DM (2011) State-Dependent Changes in Cortical Gain Control as Measured by Auditory Evoked Responses to Varying Intensity Stimuli. Sleep 34:1527–1537.

Plack CJ, Barker D, Prendergast G (2014) Perceptual consequences of “hidden” hearing loss. Trends Hear 18:233121651455062 Available at: http://journals.sagepub.com/doi/10.1177/2331216514550621 [Accessed June 1, 2020].

Rabang CF, Parthasarathy A, Venkataraman Y, Fisher ZL, Gardner SM, Bartlett EL (2012) A computational model of inferior colliculus responses to amplitude modulated sounds in young and aged rats. Front Neural Circuits 6:77.

Race N, Lai J, Shi R, Bartlett EL (2017) Differences in postinjury auditory system pathophysiology after mild blast and nonblast acute acoustic trauma. J Neurophysiol 118:782–799.

Rafaels K, “Dale” Bass CR, Salzar RS, Panzer MB, Woods W, Feldman S, Cummings T, Capehart B (2011) Survival Risk Assessment for Primary Blast Exposures to the Head. J Neurotrauma 28:2319–2328.

Remenschneider AK, Lookabaugh S, Aliphas A, Brodsky JR, Devaiah AK, Dagher

W, Grundfast KM, Heman-Ackah SE, Rubin S, Sillman J, Tsai AC, Vecchiotti M, Kujawa SG, Lee DJ, Quesnel AM (2014) Otologic outcomes after blast injury: The Boston Marathon experience. Otol Neurotol 35:1825–1834.

Ritenour AE, Wickley A, Ritenour JS, Kriete BR, Blackbourne LH, Holcomb JB, Wade CE (2008) Tympanic membrane perforation and hearing loss from blast overpressure in Operation Enduring Freedom and Operation Iraqi Freedom wounded. J Trauma 64.

Robertson D, Bester C, Vogler D, Mulders WHAM (2013) Spontaneous hyperactivity in the auditory midbrain: Relationship to afferent input. Hear Res 295:124–129.

Ryu J, Horkayne-Szakaly I, Xu L, Pletnikova O, Leri F, Eberhart C, Troncoso JC, Koliatsos VE (2014) The problem of axonal injury in the brains of veterans with histories of blast exposure. Acta Neuropathol Commun 2:153.

Säljö A, Mayorga M, Bolouri H, Svensson B, Hamberger A (2011) Mechanisms and pathophysiology of the low-level blast brain injury in animal models. Neuroimage 54:S83–S88.

Saunders GH, Frederick MT, Arnold M, Silverman S, Chisolm TH, Myers P (2015) Auditory difficulties in blast-exposed veterans with clinically normal hearing. J Rehabil Res Dev 52:343–360.

Shearer DE, Molis MR, Bennett KO, Leek MR (2018) impaired listeners by normal-hearing and hearing-impaired listeners a). 378.

Simpson G V., Knight RT, Brailowsky S, Prospero-Garcia O, Scabini D (1985) Altered peripheral and brainstem auditory function in aged rats. Brain Res

348:28–35.

Skoe E, Kraus N (2010) Auditory Brain Stem Response to Complex Sounds: A Tutorial. Ear Hear 31:302–324.

Song S, Race NS, Kim A, Zhang T, Shi R, Ziaie B (2015) A Wireless Intracranial Brain Deformation Sensing System for Blast-Induced Traumatic Brain Injury. Sci Rep 5:1–10.

Sosa MAG, De Gasperi R, Paulino AJ, Pricop PE, Shaughness MC, Maudlin-Jeronimo E, Hall AA, Janssen WGM, Yuk FJ, Dorr NP, Dickstein DL, McCarron RM, Chavko M, Hof PR, Ahlers ST, Elder GA (2014) Blast overpressure induces shear-related injuries in the brain of rats exposed to a mild traumatic brain injury. Acta Neuropathol Commun 2:1.

Sullivan S, Eucker SA, Gabrieli D, Bradfield C, Coats B, Maltese MR, Lee J, Smith C, Margulies SS (2015) White matter tract-oriented deformation predicts traumatic axonal brain injury and reveals rotational direction-specific vulnerabilities. Biomech Model Mechanobiol 14:877–896.

Sun W, Deng A, Jayaram A, Gibson B (2012) Noise exposure enhances auditory cortex responses related to hyperacusis behavior. Brain Res 1485:108–116.

Šuta D, Rybalko N, Pelánová J, Popelář J, Syka J (2011) Age-related changes in auditory temporal processing in the rat. Exp Gerontol 46:739–746.

Swaminathan J, Krishnan A, Gandour JT (2008) Pitch encoding in speech and nonspeech contexts in the human auditory brainstem. Neuroreport 19:1163–1167.

Syka J, Rybalko N (2000) Threshold shifts and enhancement of cortical evoked responses after noise exposure in rats. Hear Res 139:59–68.

Tichko P, Skoe E (2017) Frequency-dependent fine structure in the frequency-following response: The byproduct of multiple generators. Hear Res 348:1–15.

Tukey JW (1949) Comparing Individual Means in the Analysis of Variance. Biometrics 5:99.

Unnikrishnan G, Mao H, Sundaramurthy A, Bell ED, Yeoh S, Monson K, Reifman J (2019) A 3-D Rat Brain Model for Blast-Wave Exposure: Effects of Brain Vasculature and Material Properties. Ann Biomed Eng 47:2033–2044.

Valderrama JT, Beach EF, Yeend I, Sharma M, Van Dun B, Dillon H (2018) Effects of lifetime noise exposure on the middle-age human auditory brainstem response, tinnitus and speech-in-noise intelligibility. Hear Res 365:36–48.

Van Haesendonck G, Van Rompaey V, Gilles A, Topsakal V, Van de Heyning P (2018) Otologic Outcomes After Blast Injury: The Brussels Bombing Experience. Otol Neurotol 39:1250–1255.

Vander Werff KR (2012) Auditory Dysfunction Among Long-Term Consequences of Mild Traumatic Brain Injury (mTBI). Perspect Hear Hear Disord Res Diagnostics 16:3.

Viana LM, O'Malley JT, Burgess BJ, Jones DD, Oliveira CACP, Santos F, Merchant SN, Liberman LD, Liberman MC (2015) Cochlear neuropathy in human presbycusis: Confocal analysis of hidden hearing loss in post-mortem tissue. Hear Res 327:78–88.

Wagner L, Plontke SK, Rahne T (2017) Perception of Iterated Rippled Noise Periodicity in Cochlear Implant Users. Audiol Neurotol 22:104–115.

Walls MK, Race N, Zheng L, Vega-Alvarez SM, Acosta G, Park J, Shi R (2016) Structural and biochemical abnormalities in the absence of acute deficits in mild primary blast-induced head trauma. J Neurosurg 124:675–686.

Walton JP (2010) Timing is everything: Temporal processing deficits in the aged auditory brainstem. Hear Res 264:63–69.

Wang H, Turner JG, Ling L, Parrish JL, Hughes LF, Caspary DM (2009) Age-related changes in glycine receptor subunit composition and binding in dorsal cochlear nucleus. Neuroscience 160:227–239.

Wang X, Lu T, Bendor D, Bartlett E (2008) Neural coding of temporal information in auditory thalamus and cortex. Neuroscience 154:294–303 Available at: http://www.pubmedcentral.nih.gov/articlerender.fcgi?artid=2751884&tool=pmcentrez&rendertype=abstract [Accessed April 1, 2014].

Yeend I, Beach EF, Sharma M (2019) Working Memory and Extended High-Frequency Hearing in Adults: Diagnostic Predictors of Speech-in-Noise Perception. Ear Hear 40:458–467.

Yeh PH, Wang B, Oakes TR, French LM, Pan H, Graner J, Liu W, Riedy G (2014) Postconcussional disorder and PTSD symptoms of military-related traumatic brain injury associated with compromised neurocircuitry. Hum Brain Mapp 35:2652–2673.

Yin TC, Voorhees JR, Genova RM, Davis KC, Madison AM, Britt JK, Cintrón-Pérez

CJ, McDaniel L, Harper MM, Pieper AA (2016) Acute Axonal Degeneration Drives Development of Cognitive, Motor, and Visual Deficits after Blast-Mediated Traumatic Brain Injury in Mice. eNeuro 3.

Yost WA (1996a) Pitch of iterated rippled noise. J Acoust Soc Am 100:511–518.

Yost WA (1996b) Pitch strength of iterated rippled noise. J Acoust Soc Am 100:3329–3335.

Fig 1

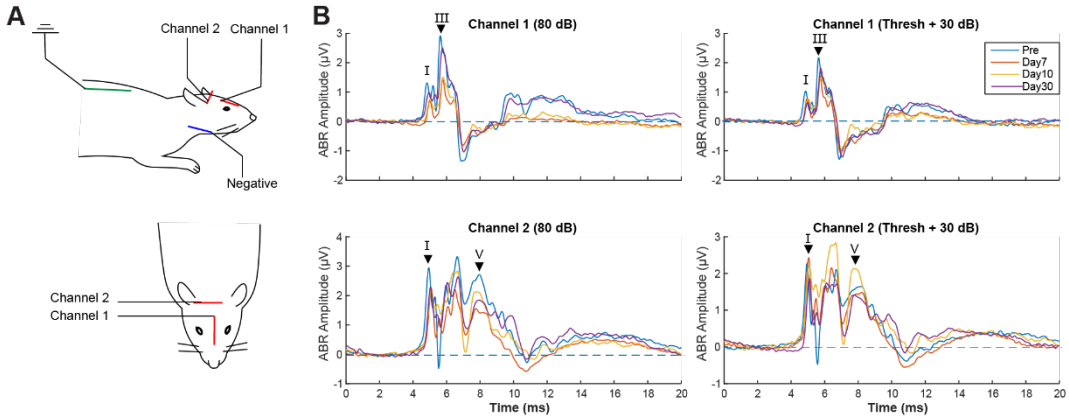

Fig 1. Auditory evoked potential experiment setup and examples of ABR waveforms. A) Electrode placement and channel configuration of the study's auditory evoked potential experiment. B) Examples of ABR waveforms at 80 dB SPL and 30 dB SL, with relevant wave peaks labeled. The waves for which amplitudes are measured are labeled with a black triangle.

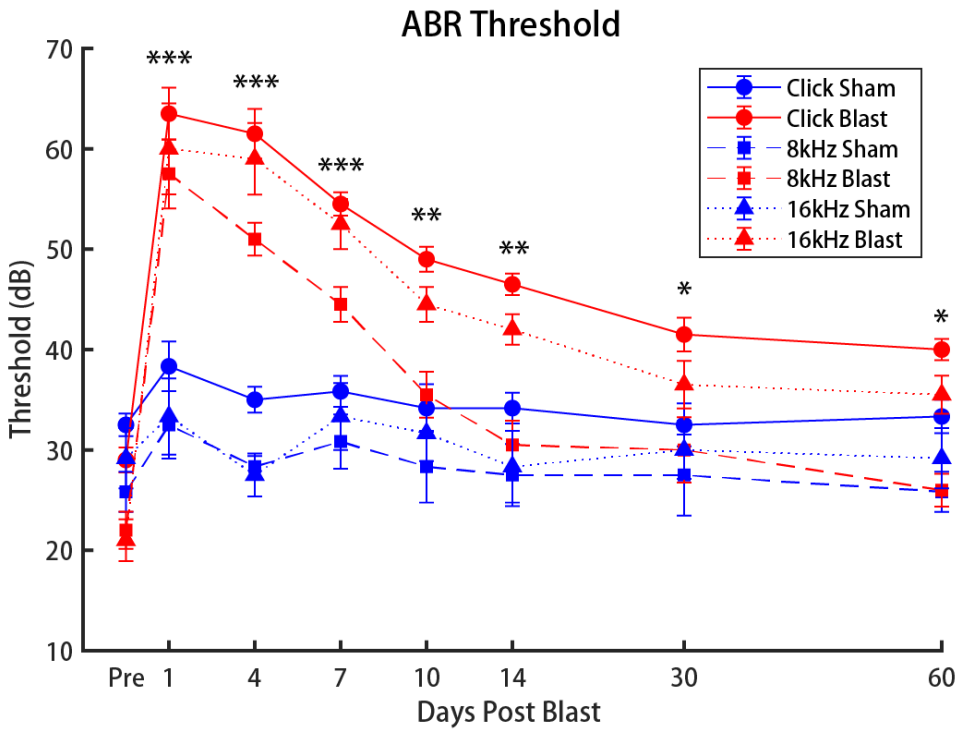

Fig 2. ABR threshold changes of Blast (N=10) and Sham (N=6) rats during the first two months post-exposure. Blast animals demonstrated drastic increases (worse) of Click, 8 kHz, and 16 kHz thresholds post-exposure as opposed to Sham animals. Significant main effects ($p \leq 0.001$) of Groups and Group*Time interactions were observed in all carriers. Significant Simple Main Effect of single time points observed in various carriers throughout the two months:

***Blast threshold significantly higher than Sham in Click, 8kHz, and 16kHz, $p<0.05$;

**Blast threshold significantly higher only in Click and 16 kHz;

*Blast threshold significantly higher only in Click.

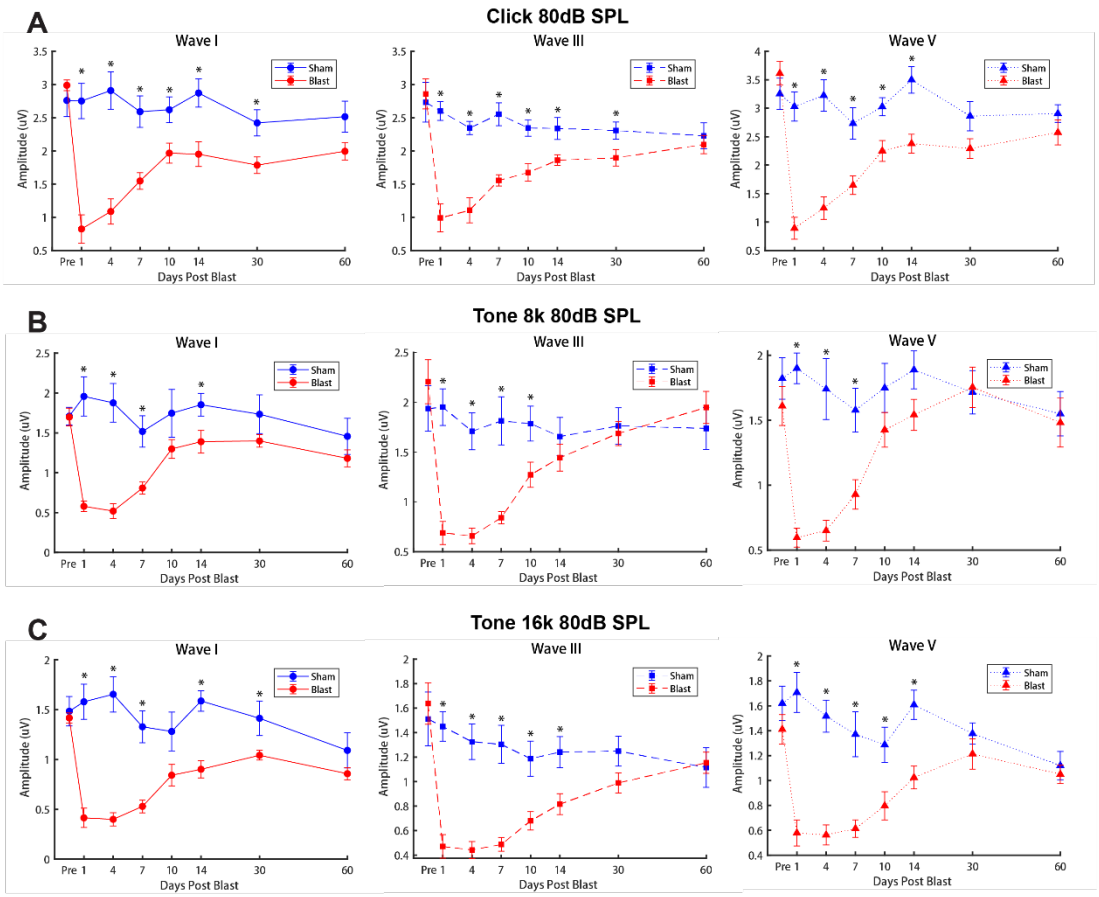

Fig 3. ABR wave I, III, and V amplitudes of Blast (N=10) and Sham (N=6) rats during the first two months post-exposure expose persistent blast-induced differences at 80 dB SPL. Significant main Group*Time interaction effects ($p \leq 0.001$) observed in all three ABR waves of all carriers: A) Click ABR; B) 8 kHz ABR; C) 16 kHz ABR. Click ABR reveals blast-induced reduction (worse) of ABR waves to a greater degree than both tone ABRs. Later waves (Wave III and V) may show earlier recovery in Blast animals.

*Significant Simple Main Effect of Group in ABR Wave Amplitudes, $p<0.05$.

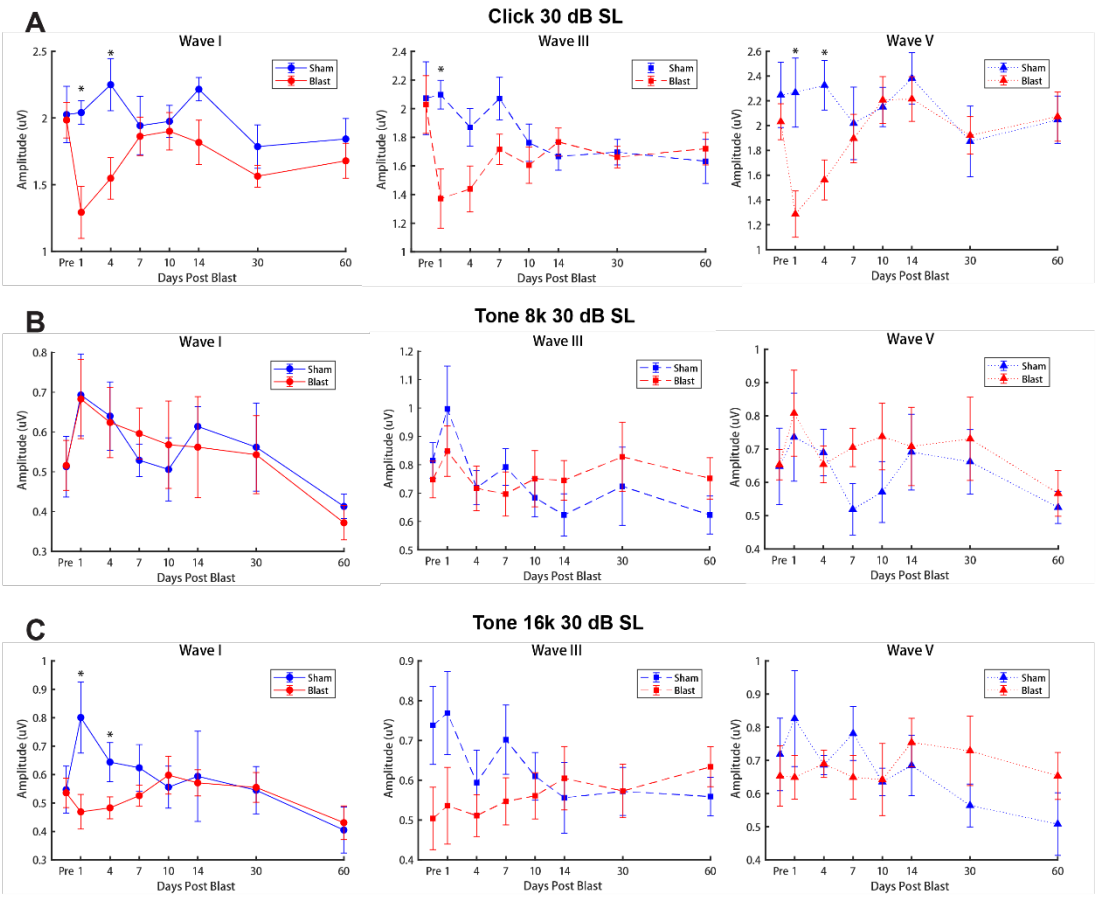

Fig 4. ABR wave I, III, and V amplitudes of Blast (N=10) and Sham (N=6) rats during the first two months post-exposure at 30 dB SL. Significant main Group*Time interaction effects only observed with Click ABR waves (Wave I: p=0.016; Wave III: p=0.04; Wave V: p=0.003) A) Click ABR; B) 8 kHz ABR; C) 16 kHz ABR.

*Significant Simple Main Effect of Group in ABR Wave Amplitudes, p<0.05.

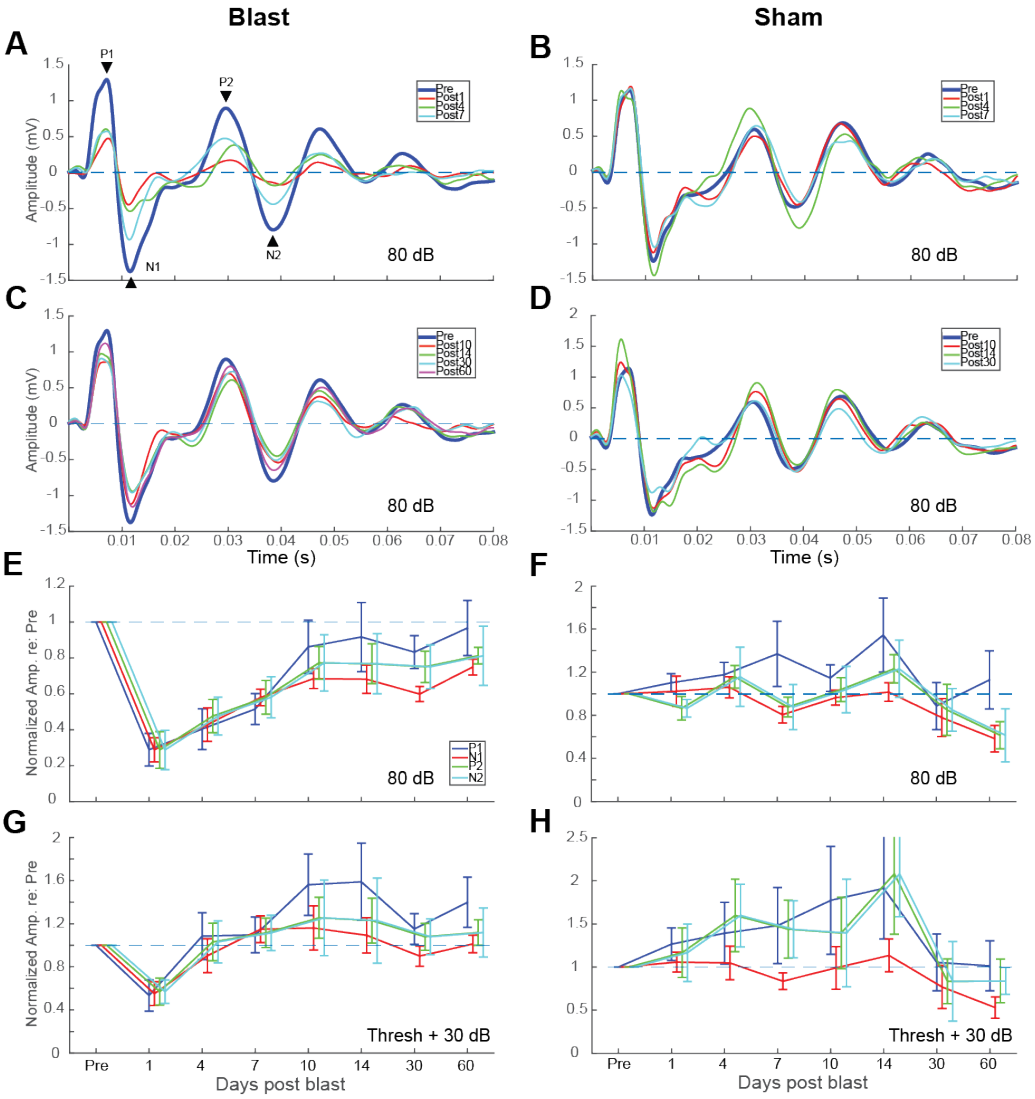

Fig 5. MLR waveforms and peak amplitudes of Blast (N=8) and Sham (N=6) rats during the first two months post-exposure at 80 dB SPL and at 30 dB SL. Grand average traces of Click MLR waveforms at 80 dB SPL: A) Blast, pre-blast to day 7; B) Sham, pre-blast to day 7; C) Blast, day 10 to day 60; D) Sham, day 10 to day 60. Normalized Click MLR wave amplitudes over time: E) Blast, 80 dB SPL; F) Sham, 80 dB SPL; G) Blast, 30 dB SL; H) Blast, 30 dB SL.

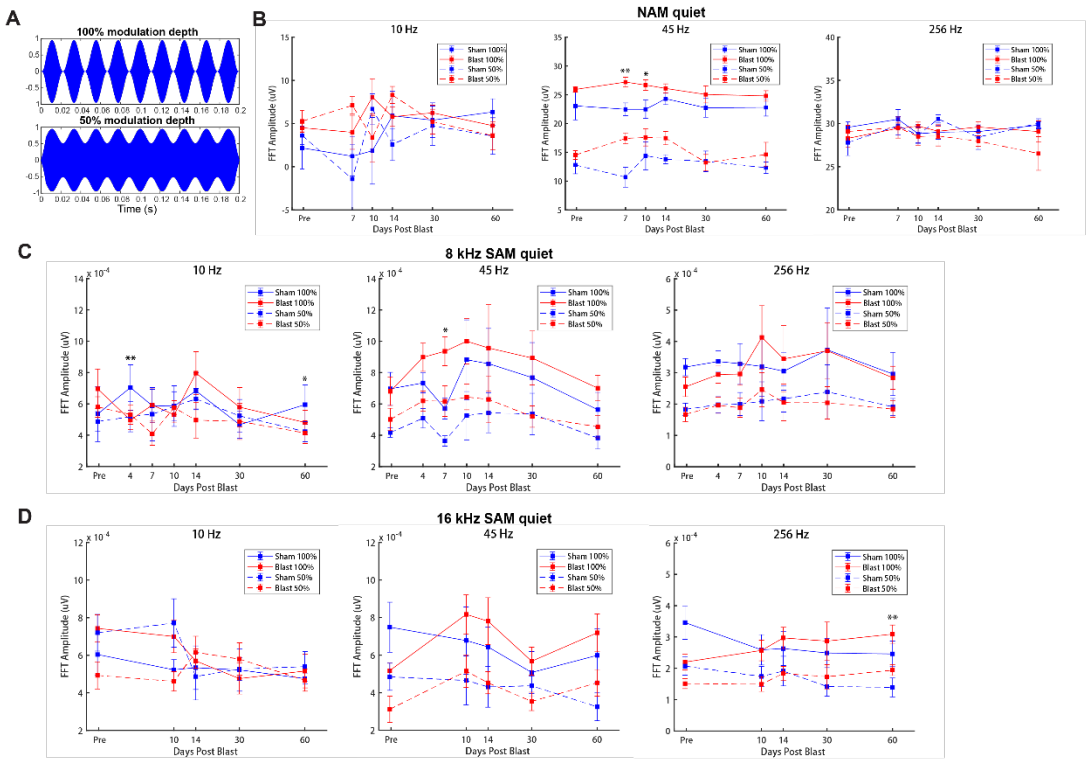

Fig 6. AM depth stimuli and EFR responses from Blast (N=10) and Sham (N=6) rats during the first two months post-exposure at 30 dB above threshold, in quiet. A) AM depth stimulus waveforms at 100% and 50% modulation depths; B) NAM FFT amplitudes showed significant Group effect at 45Hz (p=0.007); C) SAM 8 kHz FFT amplitudes at 45 Hz show a steady yet insignificant increase in later short-term (day 7-14); D) SAM 16k FFT amplitudes found no significant Group effect.

**Significant Simple Main Effect of Group in FFT Amplitudes in both 100% depth and 50% depth

* Significant Simple Main Effect of Group in FFT Amplitudes only in 100% depth

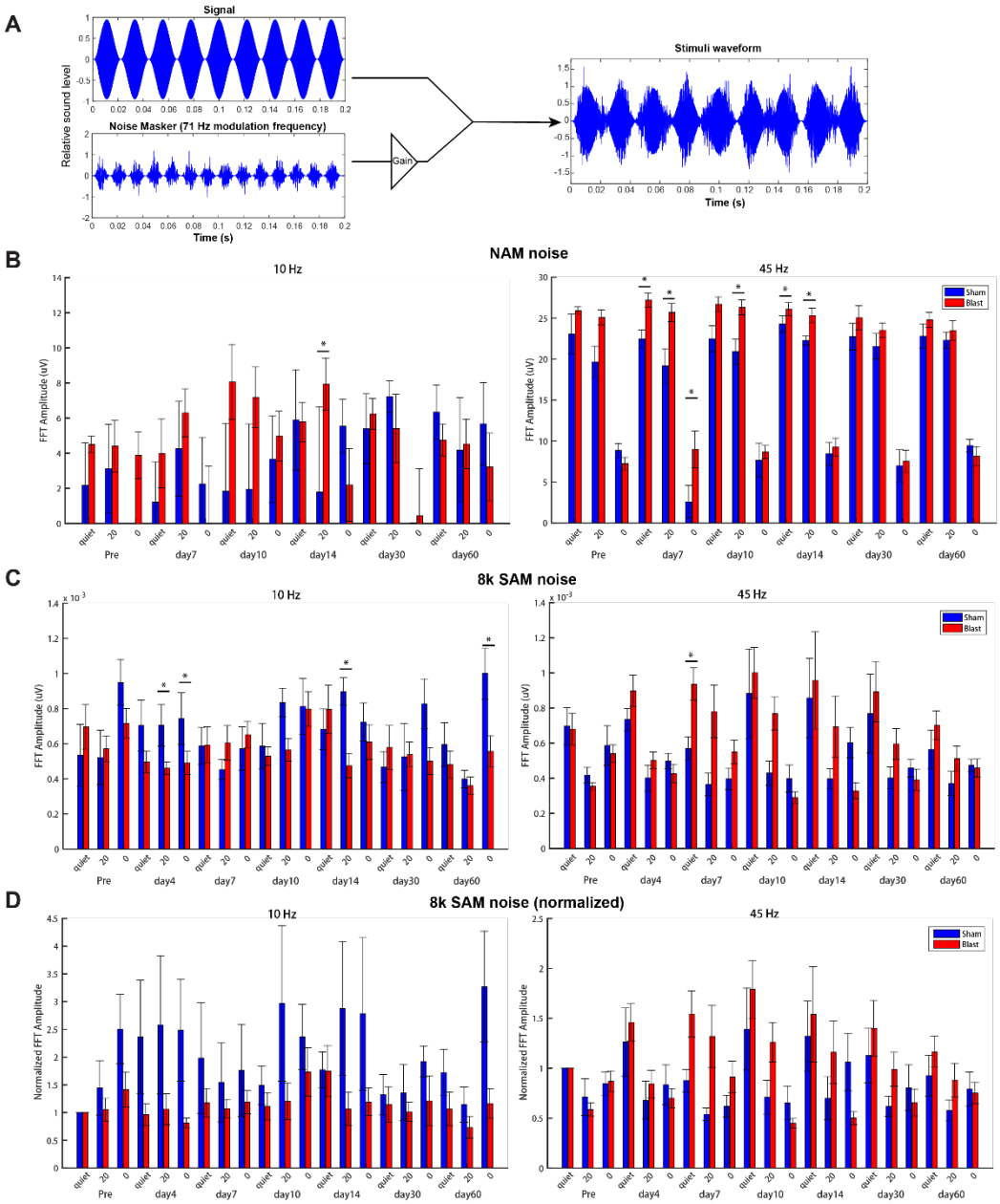

Fig 7. AM noise stimuli and EFR responses from Blast (N=10) and Sham (N=6) rats during the first two months post-exposure at 30 dB above threshold. A) AM noise stimuli composition and waveform. FFT amplitudes at signal modulation frequency in quiet and with noise masker level of 20SNR or 0SNR (equal) show significant Noise * Group effect for : B) NAM noise at 45 Hz (p=0.011) modulation frequency; C) SAM 8 kHz noise at 10 Hz (p=0.001) and 45 Hz (p=0.015) modulation frequency, and D) remained strong for 8 kHz after normalization (10 Hz: p=0.018; 45 Hz: p=0.008)

* Significant Simple Main Effect of Group

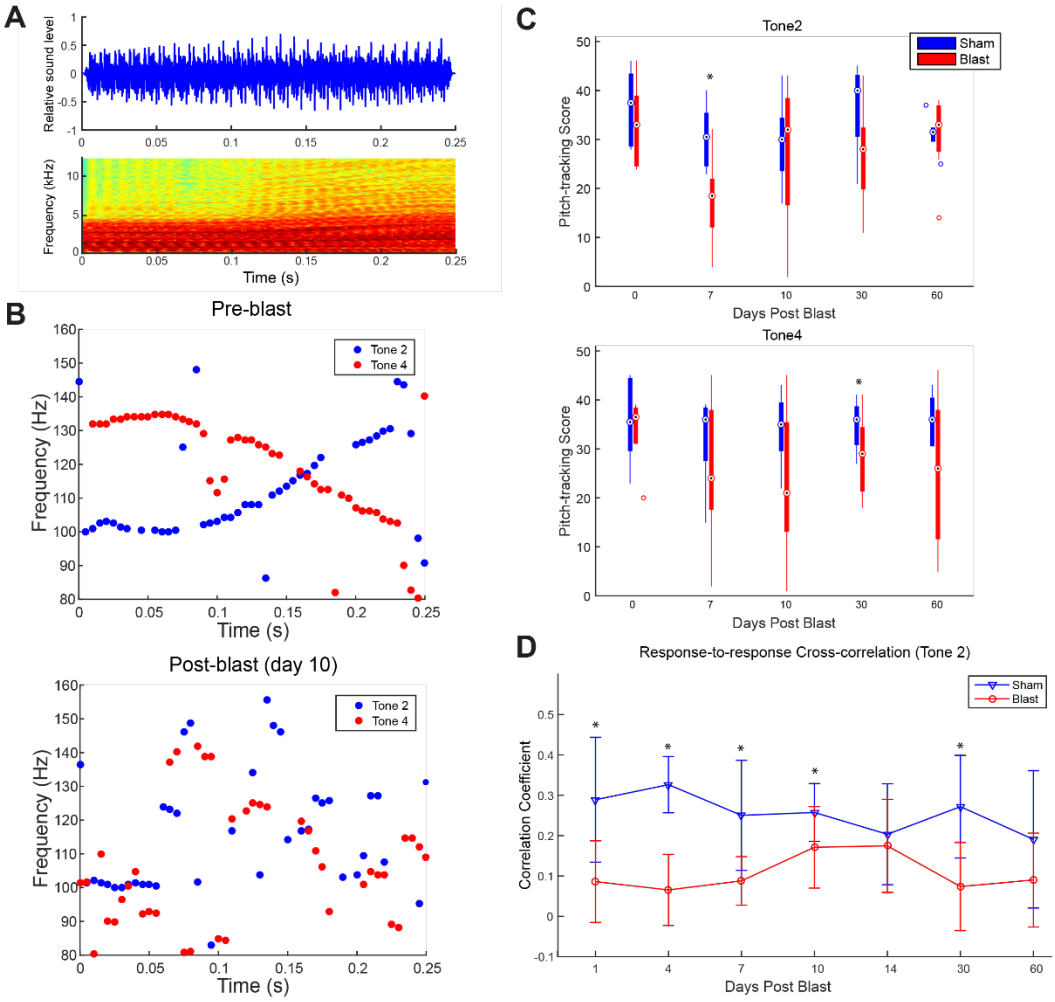

Fig 8. IRN Chinese Tone stimuli and responses from Blast (N=8) and Sham (N=6) rats during the first two months post-exposure at 30 dB above threshold A) Example waveform and spectrogram of IRN Tone 2 stimulus; B) Examples of Peak Frequency of IRN Evoked Potential in Pre-blast and Post-blast Brain; C) Significant effect of Group (*) was seen in IRN Tone 2 (p=0.026) and Tone 4 (p=0.029) pitch-tracking score, though Simple Main Effect of is limited for individual time points; D) Cross-correlation of post-blast IRN responses to corresponding pre-blast responses. Significant differences (*) in correlation coefficients to pre-blast responses between Blast and Sham were observed in two waves: day 1-10, and day 30 ($p<0.05$, paired sign-rank).

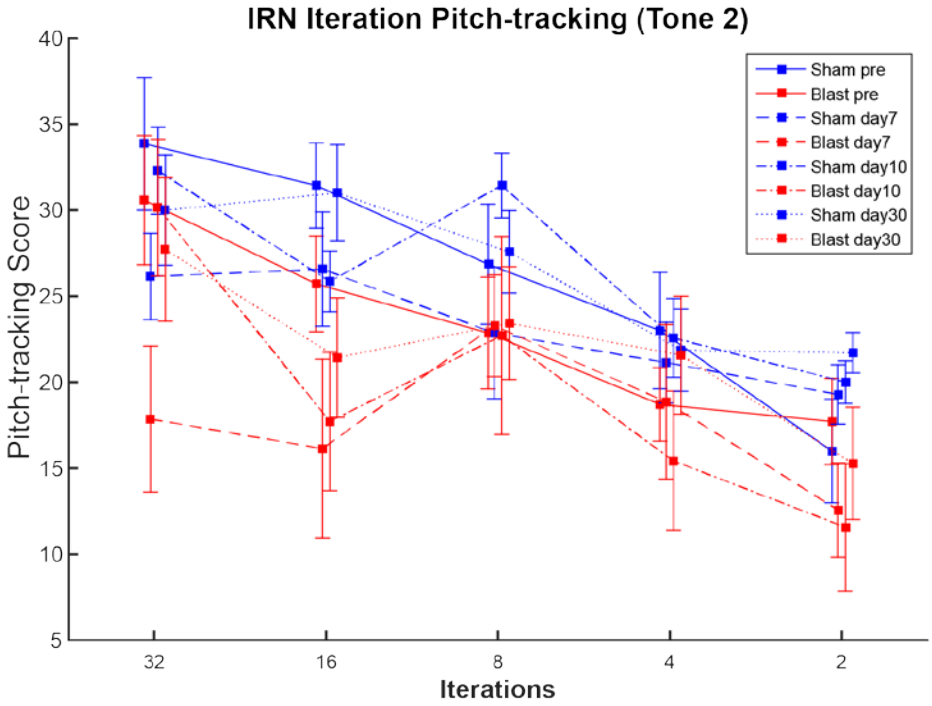

Fig 9. Responses towards IRN Tone 2 stimuli with reduced saliency (fewer iterations) from Blast (N=8) and Sham (N=6) rats at different time points, at 30 dB above threshold. Though the effect of Iterations on pitch-tracking score was significant ($p<0.001$), no significant Iteration * Group interaction was observed.

Table 1

80dB ABR			F	p	η^2_p
Click	Wave I	Time	9.980	< .001	0.416
		Group	23.080	< .001	0.622
		Time * Group	11.685	< .001	0.455
	Wave III	Time	11.065	< .001	0.441
		Group	17.207	< .001	0.551
		Time * Group	8.871	< .001	0.388
	Wave V	Time	14.134	< .001	0.502
		Group	23.203	< .001	0.624
		Time * Group	10.990	< .001	0.440
8 kHz	Wave I	Time	8.102	< .001	0.367
		Group	14.409	0.002	0.507
		Time * Group	11.760	< .001	0.457
	Wave III	Time	14.084	< .001	0.501
		Group	6.266	0.025	0.309
		Time * Group	13.826	< .001	0.497
	Wave V	Time	8.545	< .001	0.379

		Group	9.859	0.007	0.413
		Time * Group	9.346	< .001	0.400
16 kHz	Wave I	Time	9.845	< .001	0.413
		Group	27.486	< .001	0.663
		Time * Group	14.328	< .001	0.506
	Wave III	Time	9.845	< .001	0.413
		Group	13.048	0.003	0.482
		Time * Group	14.328	< .001	0.506
	Wave V	Time	8.838	< .001	0.387
		Group	20.528	< .001	0.595
		Time * Group	10.066	< .001	0.418

Table 2

Thresh + 30dB ABR			F	p	η^2_p
Click	Wave I	Time	2.554	0.019	0.154
		Group	3.637	0.077	0.206
		Time * Group	2.630	0.016	0.158
	Wave III	Time	2.544	0.052	0.154
		Group	1.811	0.200	0.115
		Time * Group	2.720	0.040	0.163
	Wave V	Time	2.568	0.018	0.155
		Group	1.479	0.244	0.096
		Time * Group	3.429	0.003	0.197
8 kHz	Wave I	Time	3.146	0.018	0.183
		Group	6.852e -5	0.994	0.000
		Time * Group	0.200	0.945	0.014
	Wave III	Time	2.432	0.069	0.148
		Group	0.020	0.889	0.001
		Time * Group	1.184	0.328	0.078
	Wave V	Time	1.837	0.136	0.116

		Group	0.361	0.558	0.025
		Time * Group	0.618	0.648	0.042
16 kHz	Wave I	Time	2.325	0.031	0.142
		Group	1.046	0.324	0.070
		Time * Group	2.381	0.027	0.145
	Wave III	Time	0.562	0.651	0.039
		Group	1.149	0.302	0.076
		Time * Group	1.930	0.136	0.121
	Wave V	Time	1.160	0.338	0.077
		Group	4.905e -4	0.983	0.000
		Time * Group	1.646	0.161	0.105